Science Advances
AAAS

Supplementary Materials for

RNA polymerase II is required for spatial chromatin reorganization following exit from mitosis

Shu Zhang, Nadine Übelmesser, Natasa Josipovic, Giada Forte, Johan A. Slotman, Michael Chiang, Henrike Johanna Gothe, Eduardo Gade Gusmao, Christian Becker, Janine Altmüller, Adriaan B. Houtsmuller, Vassilis Roukos, Kerstin S. Wendt, Davide Marenduzzo, Argyris Papantonis*

*Corresponding author. Email: argyris.papantonis@med.uni-goettingen.de

Published 22 October 2021, *Sci. Adv.* **7**, eabg8205 (2021)
DOI: 10.1126/sciadv.abg8205

The PDF file includes:

Figs. S1 to S8
Tables S1, S3 and S4
Legends for tables S2 and S5

Other Supplementary Material for this manuscript includes the following:

Tables S2 and S5

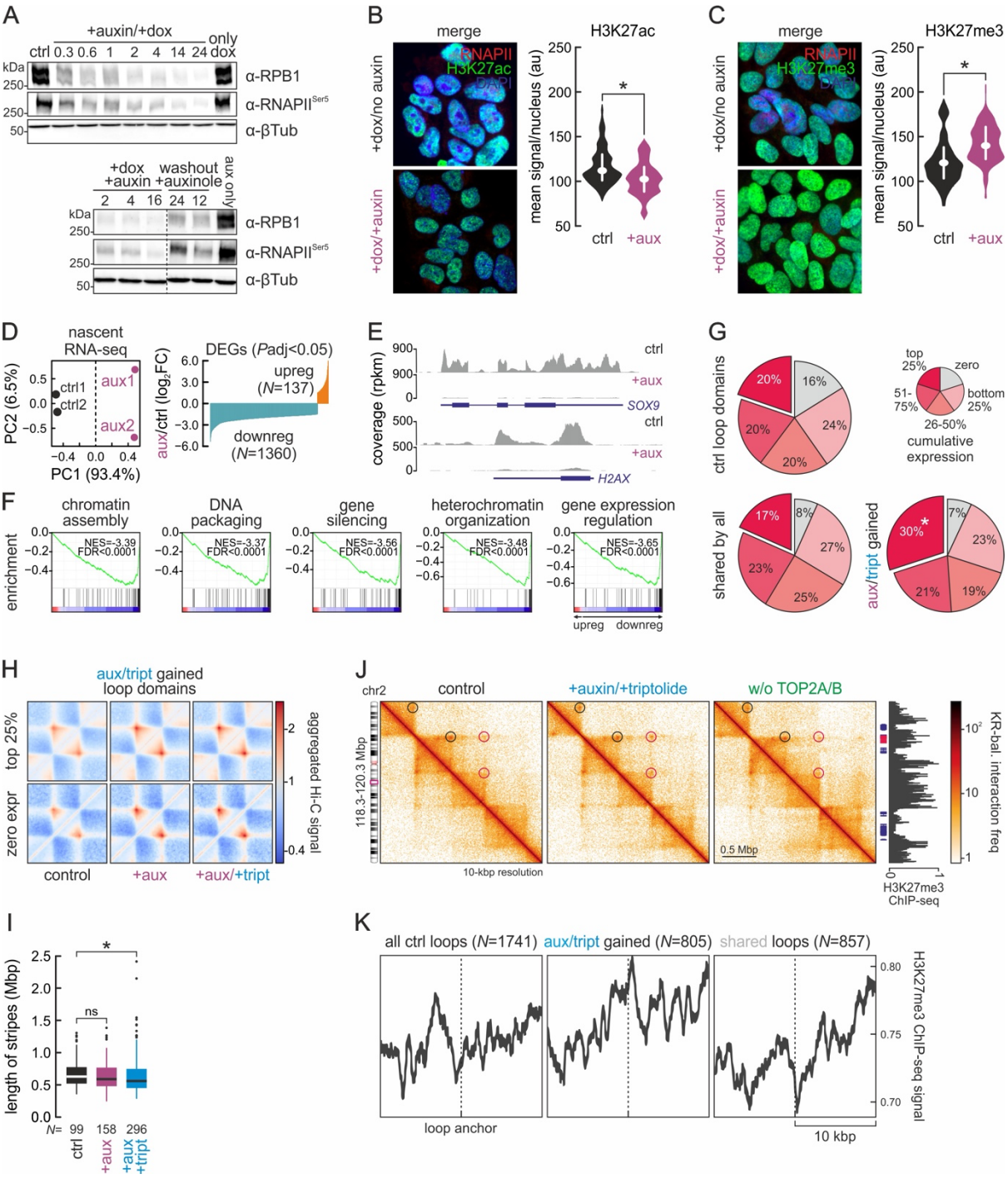

Fig. S1. RNAPII degradation, recovery and its effects on interphase chromatin folding. (**A**) Western blots showing depletion of total cell RPB1 or phospho-Ser5-RNAPII on increasing exposure to doxycycline plus auxin (top) or RNAPII recovery following auxin washout in the presence of auxinole (bottom); β-tubulin provides a loading control. (**B**) Representative H3K27ac immunofluorescence from untreated (top) or 14-h auxin-treated cells (bottom) and signal quantification (bean plots). *: significantly different; $P<0.01$, Wilcoxon-Mann-Whitney test. Bar: 5 μM. (**C**) As in panel B, but for H3K27me3 levels. (**D**) *Left*: PCA plot for G1-sorted control (black) and 14-h auxin-treated nascent RNA-seq data (purple). *Right*: Nascent RNA changes (log_2 fold-change compared to control; $P_{adj}<0.05$) in 1497 genes upon auxin treatment. (**E**) Genome browser examples of nascent RNA reduction at two typical gene loci. (**F**) Gene set enrichment analysis of data in panel D; top five enriched pathways. (**G**) Pie charts showing

distribution of all (top), shared (bottom left) and auxin/triptolide-shared loops (bottom right) according to their cumulative gene expression levels (no expression – grey; four nonoverlapping quantiles – shades of red). *: significantly different; $P<0.05$, Fisher's exact test. (**H**) Heatmaps showing mean loop domain interactions in control (top), auxin- (middle) and auxin-/triptolide-treated cells (bottom) for the auxin/triptolide-shared loops of panel G. (**I**) Boxplots showing changes in the length of stripes detected in Hi-C data from control (black), auxin-treated (purple) or auxin/triptolide-treated Hi-C data (blue). *: significantly different to control; $P<0.05$, Wilcoxon-Mann-Whitney test. (**J**) Hi-C maps from control (left), auxin/triptolide-treated (middle) or TOP2A/B-depleted cells (right) in the chr2 subregion encompassing the *HOXD* gene cluster. H3K27me3 ChIP-data from control cells are aligned to the maps, and emerging H3K27me3-anchored loops are denoted (red circles). (**K**) Line plots showing mean H3K27me3 ChIP-seq signal enrichment in the 20 kbp around all (left), auxin-/triptolide-gained loops (middle) or loops shared between RNAPII-depleted and control cells (right). The number of loops in each group (*N*) is indicated. The Hi-C data presented and analyzed in panels H-K come from individual Hi-C replicates (see Table S1).

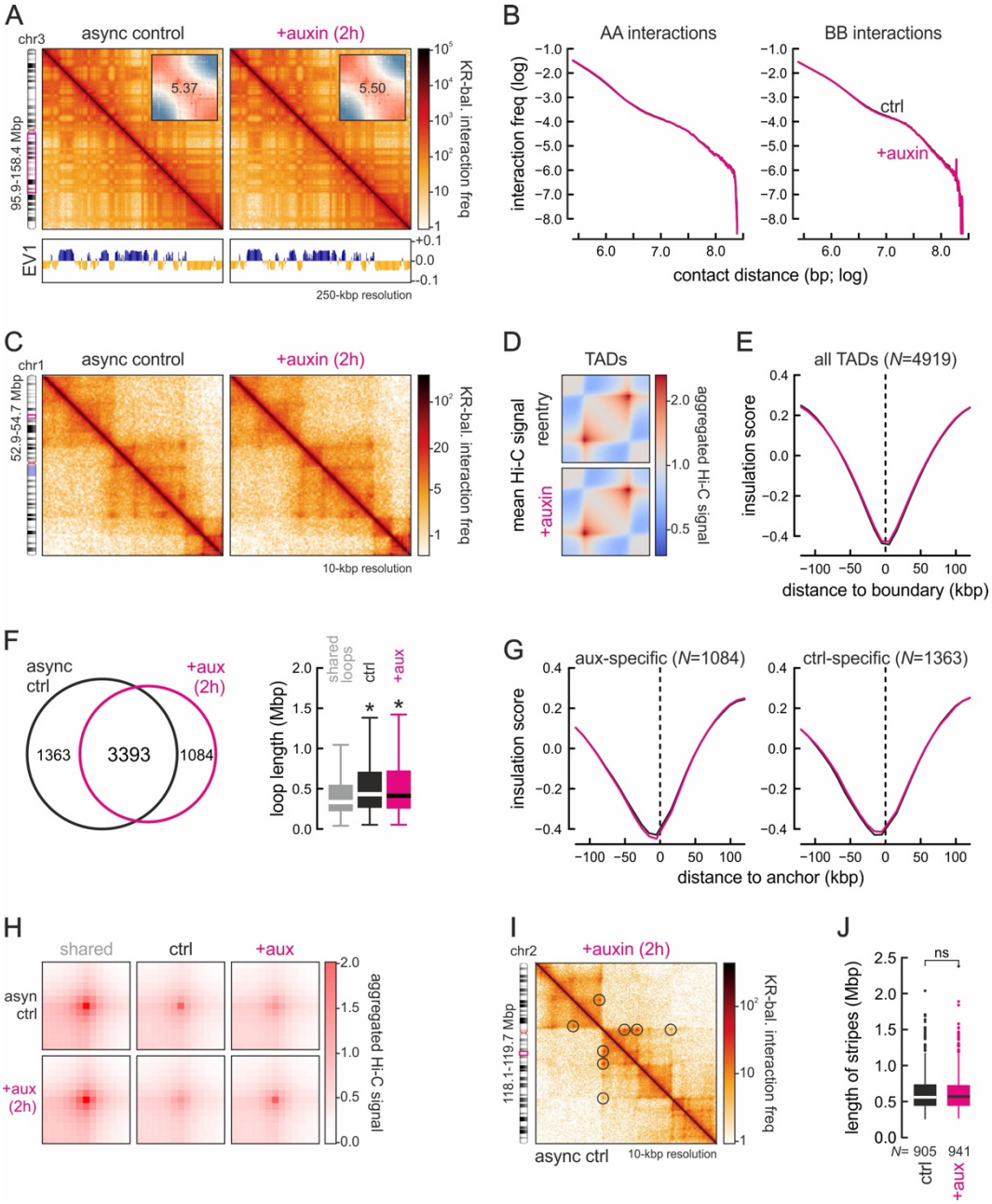

Fig. S2. Short-term RNAPII degradation does not affect G1-phase chromatin folding. (**A**) Exemplary Hi-C maps of a subregion of chr3 from asynchronous control (left) and 2-h auxin-treated DLD1-mAID-RPB1 cells (right) at 250-kbp resolution aligned to first eigenvector values (EV1; below). *Insets*: saddle plots showing no change in A/B-compartment insulation. (**B**) Decay plots showing Hi-C interaction frequency between A- (left) or B-compartments (right) as a function of genomic distance (log) in control (black line) and 2-h auxin-treated cells (magenta line). (**C**) Exemplary Hi-C maps of a subregion of chr1 from control (left) and auxin-treated cells (right) at 10-kbp resolution. (**D**) Heatmaps showing aggregated TAD-level interactions in control (top) and auxin-treated cells (bottom). (**E**) Line plots showing mean insulation score from control (black line) and auxin-treated cells (magenta line) in the 240 kbp around all TAD boundaries in control cells. The number of TAD boundaries queried (*N*) is indicated. (**F**) *Left*: Venn diagram showing shared and unique loops in control (black) and auxin-treated Hi-C data (magenta). *Right*: Loop lengths displayed as boxplots. *: significantly different; $P<0.01$, Wilcoxon-Mann-Whitney test. (**G**) As in panel E, but for the anchors of control- (left) and degron-specific loops (right; from panels

H,I). (**H**) Aggregate plots showing mean Hi-C signal at shared (left), control- (middle), and degron-specific loops (right) from panel F. (**I**) Composite Hi-C map showing little change in loop emergence (circles) between control (bottom half) and auxin-treated cells (top half). (**J**) Boxplots showing no significant change in the length of stripes detected in Hi-C data from control (black) or auxin-treated cells (magenta). The Hi-C data presented and analyzed in panels A-J come from individual Hi-C replicates (see Table S1).

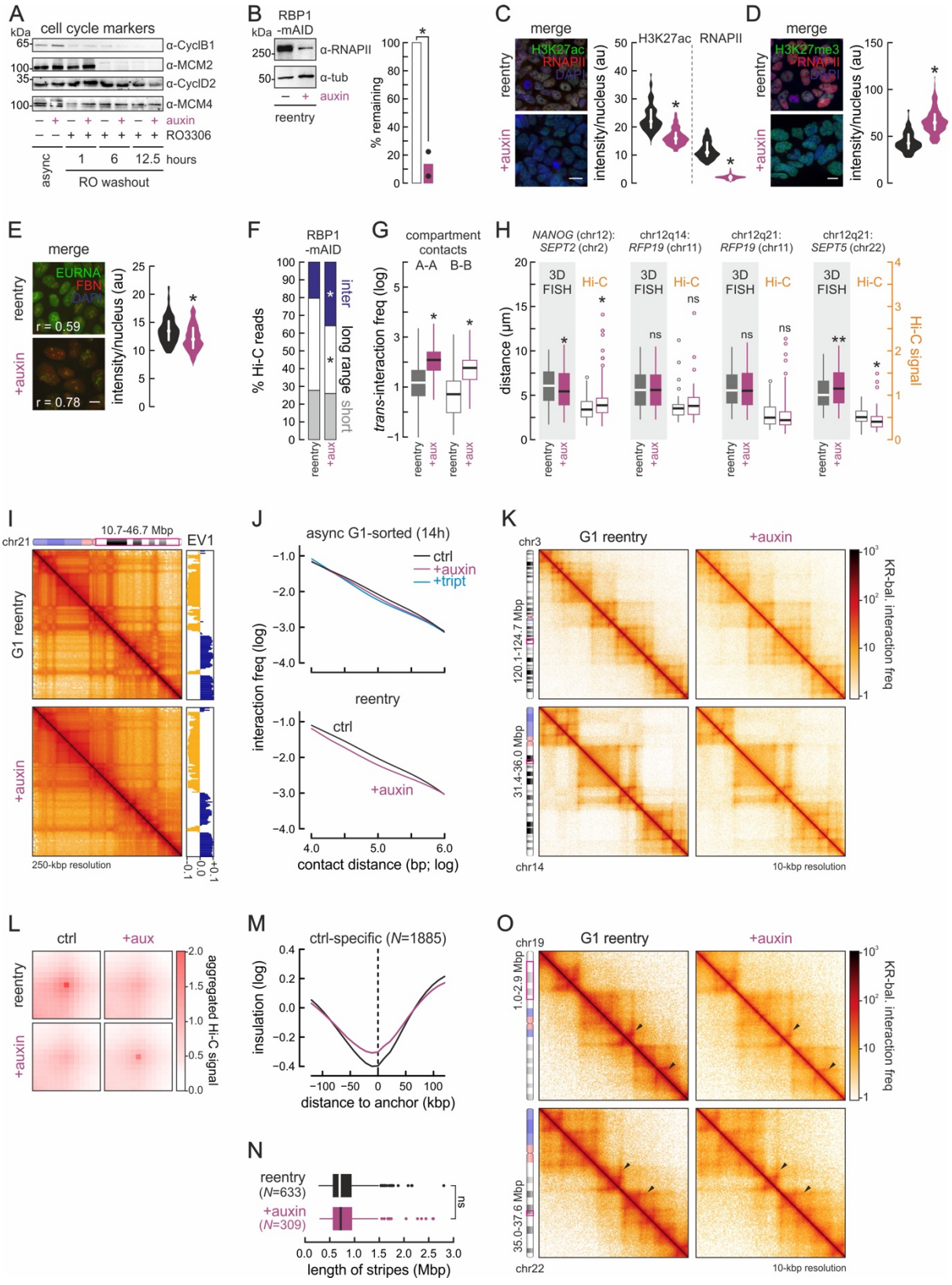

Fig. S3. RNAPII degradation affects chromatin refolding in *cis* and in *trans* following mitosis. (**A**) Western blots of selected cell cycle markers in cells treated or not with auxin at different times after release from the G2/M block. (**B**) *Left*: Western blot of RNAPII (RPB1) in G1-reentry cells treated or not with auxin; β-tubulin provides a loading control. *Right*: Quantification of such western blot data from two

independent replicates. *: significantly different mean; *P*<0.01, unpaired two-tailed Student's t-test. (**C**) *Left*: Exemplary widefield immunofluorescence images of DLD1-mAID-RPB1 G1-reentry cells treated with doxycycline plus auxin (bottom) or not (top) and stained for H3K27ac and RNAPII (RPB1); nuclei were counterstained with DAPI. *Right*: Bean plots showing mean fluorescence intensity per nucleus. *: significantly different; *P*<0.01, Wilcoxon-Mann-Whitney test. (**D**) As in panel C, but stained for RNAPII and H3K27me3, and quantifying H3K27me3 levels. (**E**) As in panel C, but stained for fibrillin and EU-labeled nascent RNA, and quantifying EU-RNA levels. The correlation of signal from the two fluorescent channels (r) is also indicated. (**F**) Bar plots showing percent of Hi-C reads in inter- (blue), long-range (>20 kbp) or short-range intra-chromosomal contacts (white) across datasets. *: significantly different; *P*<0.01, Fisher's exact test. (**G**) Boxplots showing inter-chromosomal interactions between A-A and B-B compartments in auxin-treated versus control reentry cells. *: significantly different; *P*<0.01, Wilcoxon-Mann-Whitney test. (**H**) Boxplots comparing interchromosomal distance changes for the loci indicated assessed using high throughput 3D-DNA FISH (grey background) or Hi-C data at 0.5-Mbp resolution. *: significantly different; *P*<0.01, Wilcoxon-Mann-Whitney test. (**I**) Additional Hi-C examples of a subregion of chr3 from control (top) and auxin-treated reentry cells (bottom) at 250-kbp resolution aligned first eigenvector values (right). (**J**) Decay plots showing Hi-C interaction frequency as a function of genomic distance (log) at the scale of TADs (0.01-1 Mbp) in control (black line) or auxin-treated reentry cells (purple/blue lines). (**K**) Additional Hi-C examples of subregions in chr3 and 14 from control (left) and auxin-treated reentry cells (right) at 10-kbp resolution. (**L**) Plots showing aggregate Hi-C signal for loops lost/gained in control (left) and auxin-treated reentry cells (right). (**M**) Line plots showing mean insulation scores in the 240 kbp around control- (top) or degron-specific loops (bottom) from control (black line) and auxin-treated cells (purple line). The number of anchors queried (*N*) is indicated. (**N**) Boxplots showing no significant change in the length of stripes detected in Hi-C data from control (black) or auxin-treated cells (purple). (**O**) Hi-C maps showing typical changes in "stripes" (arrowheads) between control (left) and auxin-treated reentry cells (right) at 10-kbp resolution. The Hi-C data presented and analyzed in panels I-O come from two merged Hi-C replicates (see Table S1).

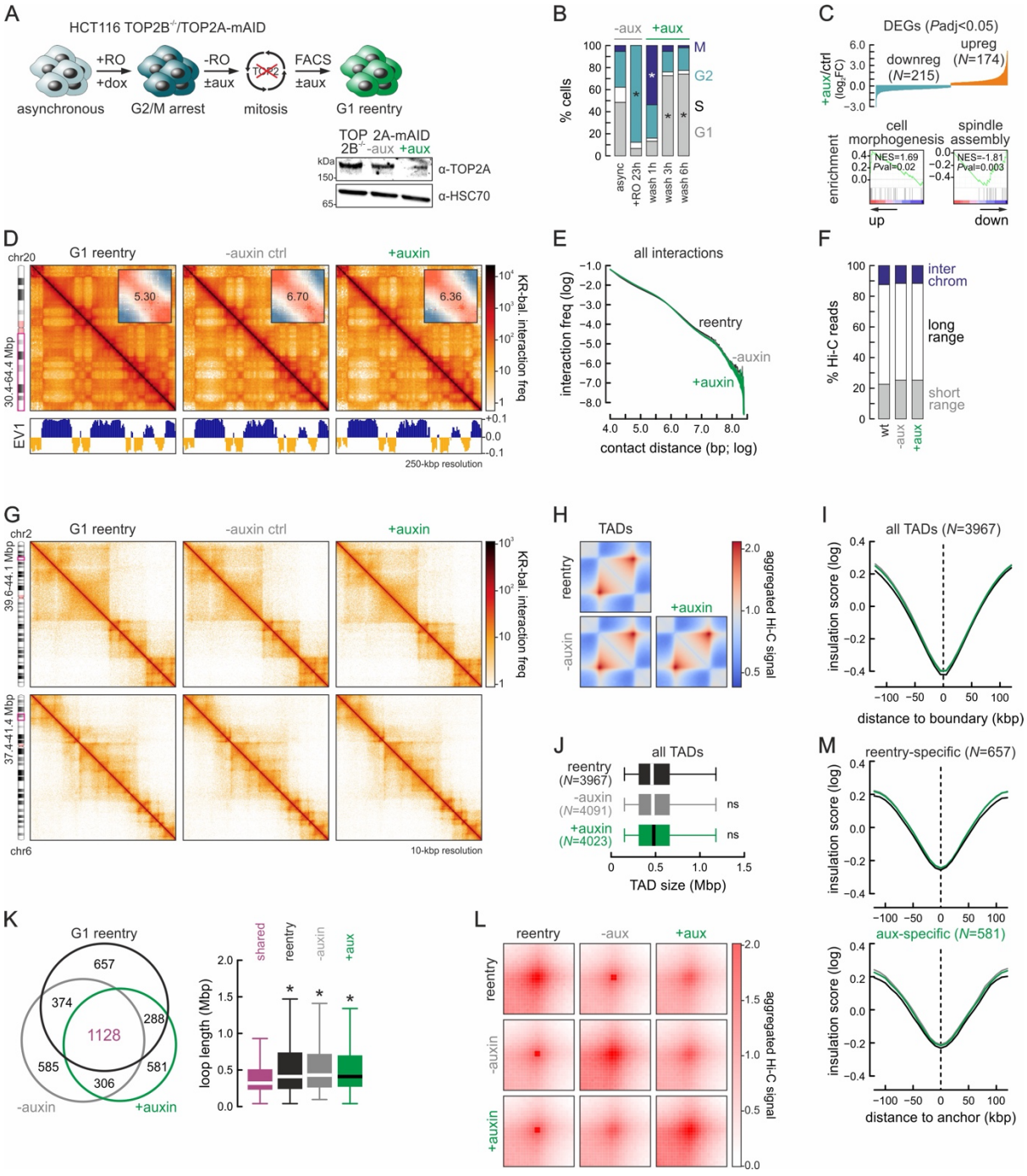

Fig. S4. Topoisomerase II depletion marginally affects chromatin refolding following mitosis. (**A**) *Top*: Overview of the experimental scheme for HCT116-TOP2B$^{-/-}$-TOP2A-mAID cell synchronization and release. *Bottom right*: Western blots showing auxin-mediated TOP2A degradation; HSC70 provides a loading control. (**B**) Bar plots showing the percent of cells in each phase from panel A. *: significantly different; P<0.01, Fisher's exact test. (**C**) *Top*: Graph showing nascent transcription changes ($\log_2$ fold-change compared to control, P_{adj}<0.05) upon TOP2-depletion. *Bottom*: Gene set enrichment analysis. (**D**) Exemplary Hi-C maps of a subregion of chr20 from control (left), TOP2B$^{-/-}$-untreated and TOP2B$^{-/-}$-auxin-treated G1-reentry cells (right) at 250-kbp resolution aligned to first eigenvector values (below). *Insets*: saddle plots showing compartment insulation. (**E**) Decay plots showing interaction frequency as a function of genomic distance (log) in the Hi-C data from panel D. (**F**) Bar plots showing the percentage

of Hi-C reads in interchromosomal (blue), long- (>20 kbp; white) and short-range intra-chromosomal contacts (grey) in the Hi-C data from panel D. (**G**) Exemplary 10-kbp resolution Hi-C maps of subregions in chr1 and 6 from the same conditions as in panel D. (**H**) Heatmaps showing aggregated TAD-level interactions in control (top), TOP2B$^{-/-}$-untreated (bottom left) and TOP2B$^{-/-}$-auxin-treated reentry cells (bottom right). (**I**) Line plots showing mean insulation scores in the 240 kbp around TAD boundaries from panel H. The number of TADs queried (*N*) is indicated. (**J**) Boxplots showing size changes in the TAD groups from panel H. (**K**) *Left*: Venn diagram showing shared and unique loops between the Hi-C datasets from panel D. *Right*: Loop lengths displayed as boxplots. *: significantly different to shared loops; $P<0.01$, Wilcoxon-Mann-Whitney test. (**L**) Plots showing aggregate Hi-C signal for the loop categories from panel K. (**M**) As in panel I, but for the anchors of loop from panels K,L. The Hi-C data presented and analyzed in panels A-M come from individual Hi-C replicates (see Table S1).

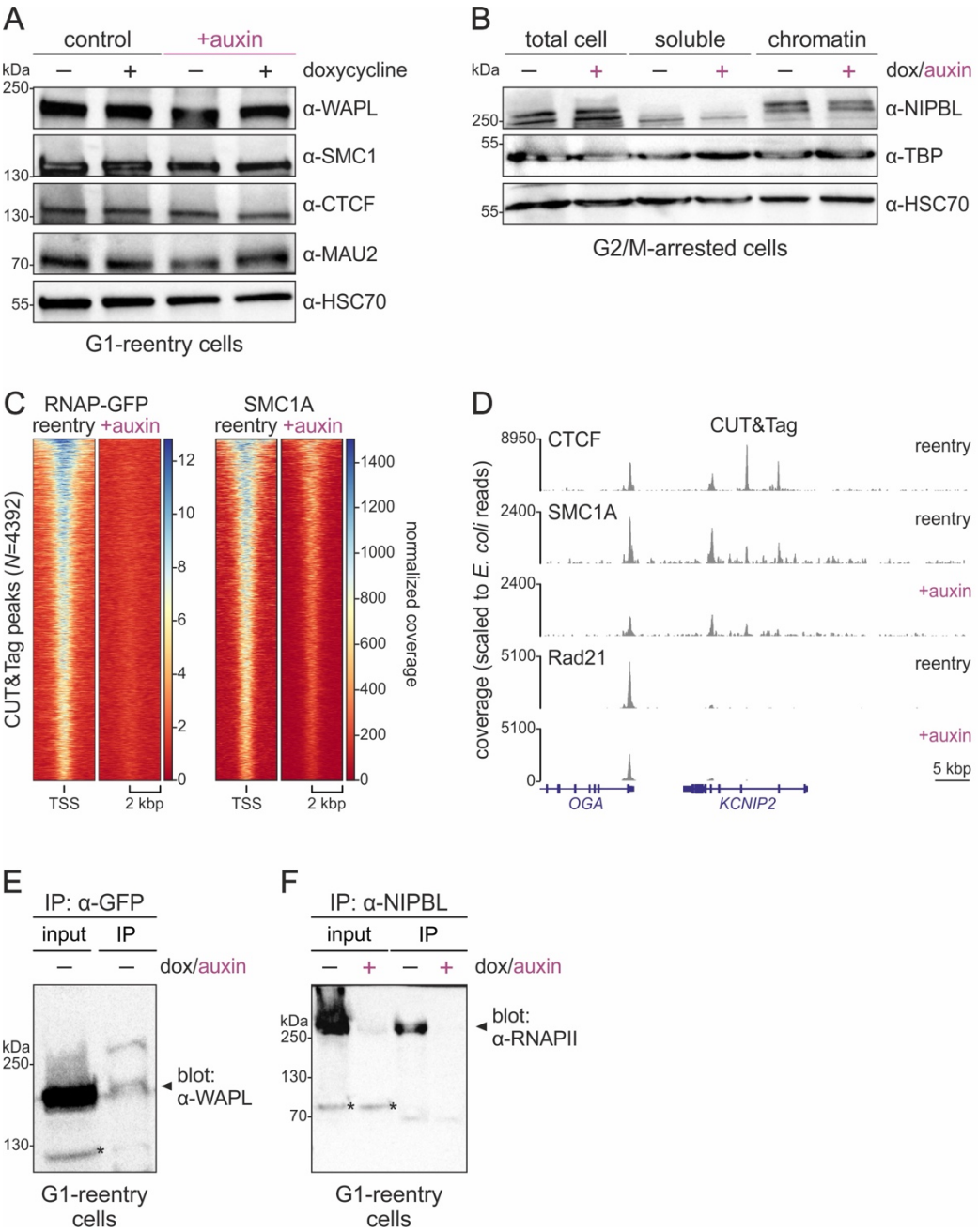

Fig. S5. RNAPII interacts with cohesin complex subunits and its depletion affects their binding to DNA. (**A**) Western blots showing unchanged cohesin components (SMC1A, MAU2, WAPL) and CTCF levels upon RNAPII degradation in G1-reentry cells; HSC70 provides a control. (**B**) Fractionation blots for NIPBL and TBP in G2/M-arrested cells treated or not with auxin; HSC70 provides a control. (**C**) Heatmaps showing scaled RNAPII (left) and SMC1A (right) CUT&Tag signal from control and auxin-treated G1-reentry cells in the 4 kbp around active TSSs. (**D**) Typical browser views of CTCF, SMC1A, and Rad21 CUT&Tag data from G1-reentry cells treated or not with auxin (merge of two replicates). (**E**) Western blot showing WAPL co-immunoprecipitating with mClover-mAID-RPB1 in G1-reentry cells. (**F**) As in panel E, but showing RNAPII (RPB1) co-immunoprecipitating with NIPBL only in untreated G1-reentry cells. *: unspecific bands.

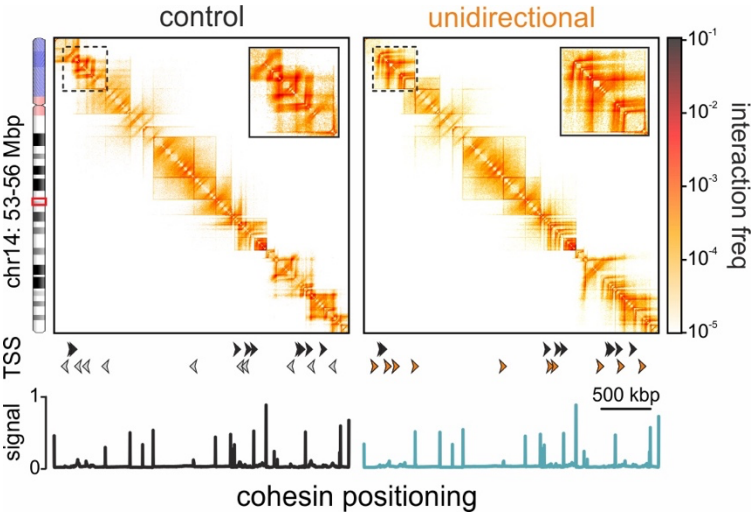

Fig. S6. The direction of transcription can affect loop extrusion. Heatmaps rendered from loop extrusion 1D simulations representing wild-type chromatin (left) or chromatin where all TSS are transcribed in the same direction (right) in the HUVEC chr14:53-56 Mbp segment. Profiles of cohesin positioning and TSS orientations are aligned below each heatmap (reoriented TSSs are indicated in orange).

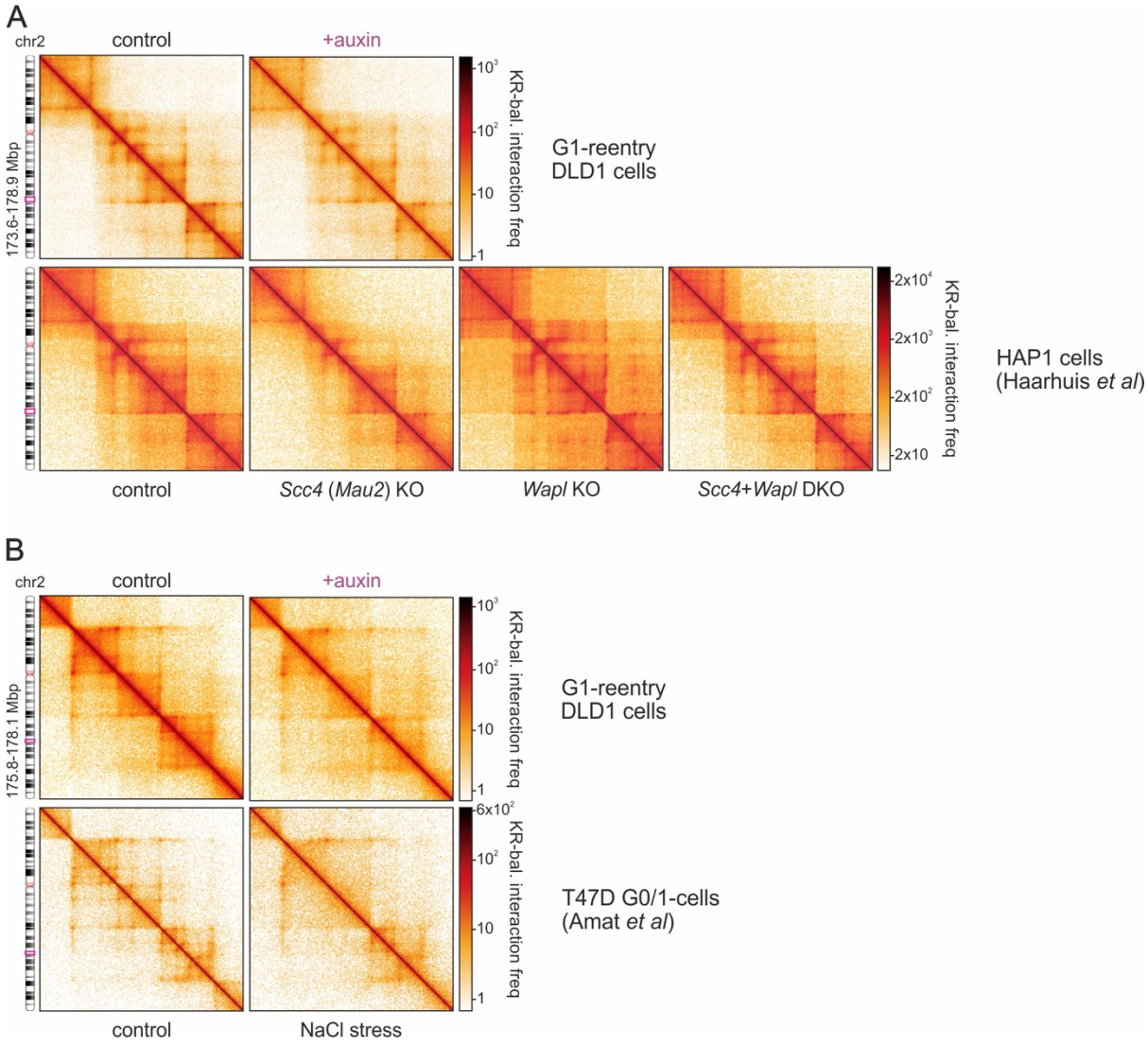

Fig. S7. Comparison of RNAPII-depletion to Wapl/Mau2-depletion or hyperosmotic stress Hi-C data. (**A**) Exemplary Hi-C heatmaps from a subregion for chr2 (ideogram) derived from G1-reentry DLD-1 (top row) compared to heatmaps from wild-type, *Scc4*-KO, *Wapl*-KO, and *Scc4*/*Wapl*-DKO HAP1 cells (bottom row; data from ref. *13*). (**B**) As in panel A, but comparing Hi-C from G1-reentry DLD-1 (top row) to data from T47D cells before and after NaCl stress (bottom row; data from ref. *60*). All Hi-C data presented here are from merged Hi-C replicates (see Table S1 and refs *13* and *60*).

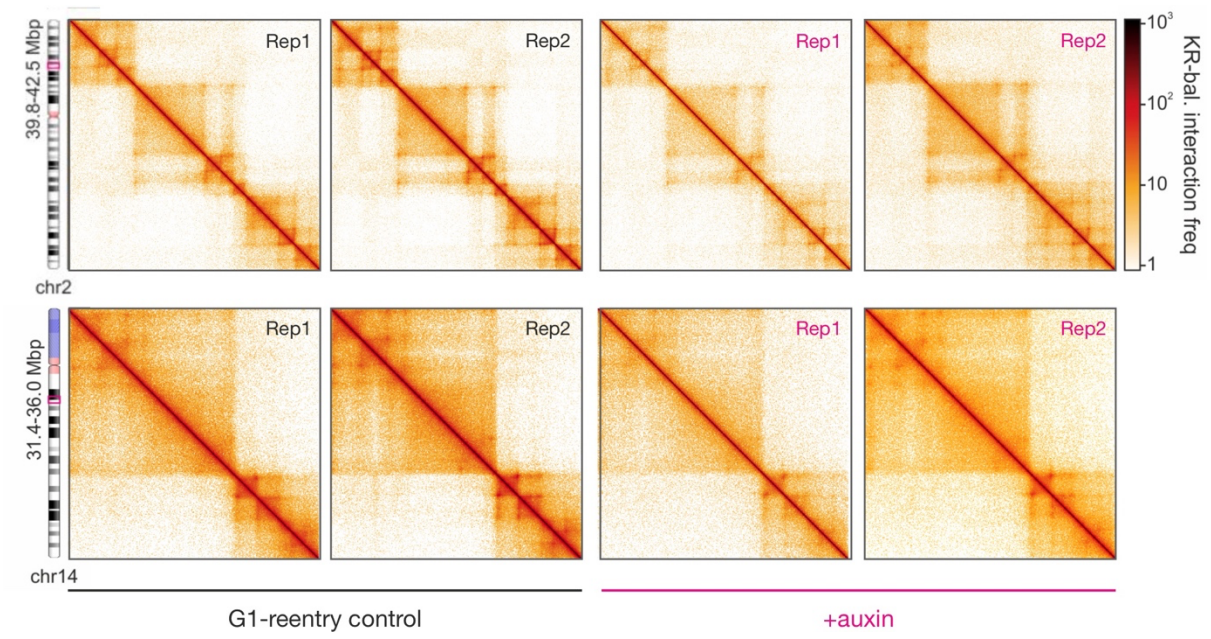

Fig. S8. Data from individual G1-reentry Hi-C replicates are reproducible. Representative Hi-C heatmaps from subregions of chr2 and 14 (ideograms) derived from independent replicates generated using G1-reentry DLD-1 cells treated (+auxin) or not with auxin (control). Details for each replicate can be found in Table S1.

Table S1. General statistics of all Hi-C datasets.

Hi-C dataset:	total reads	% aligned	Hi-C contacts	% inter-chromo	% intra-chromo	% short-range	% long-range
2h control	570,638,421	89.91	387,244,720	10.44	57.42	21.94	35.47
2h +auxin	521,206,158	91.46	361,994,319	10.84	58.62	22.43	36.17
G1 control, r1	512,551,503	89.70	339,693,791	16.49	49.78	16.75	33.03
G1 control, r2	617,136,578	89.46	400,421,522	12.40	52.48	18.77	33.70
14h +aux/+tript	461,569,471	90.67	313,489,486	16.87	51.04	19.88	28.67
14h +auxin	516,427,195	89.04	338,221,913	17.69	47.80	17.65	30.14
reentry +aux, r1	538,423,263	90.05	355,346,372	24.38	41.61	16.90	24.70
reentry +aux, r2	1,153,253,737	89.37	714,520,317	22.96	39.00	15.78	23.21
TOP2 control	705,232,509	88.87	462,507,451	12.44	53.14	22.59	30.55
TOP2 -auxin	541,077,797	88.39	364,665,469	10.32	57.07	23.96	33.11
TOP2 +auxin	546,798,121	88.24	368,526,565	10.08	57.32	24.49	32.83

Table S3. Targets of 3D-DNA FISH probes.

probe target:	genomic coordinates (hg19)
Nanog	chr12:7,696,106-7,696,694
chr12q14	chr12:60,211,422-60,211,814
chr12q21	chr12:83,646,182-83,815,279
PRPF19	chr11:60,677,496-60,677,988
SEPT2	chr2:242,097,006-242,097,495
SEPT5	chr22:19,578,750-19,579,058

Table S4. Antibodies used in Western blots.

antibody:	cat. No., provider	working dilution
anti-CTCF	61311 Active Motif	1:2,000
anti-GFP	ab290, Abcam	1:1,000
anti-H3K27ac	39133, Active Motif	1:1,000
anti-H3K27me3	39155, Active Motif	1:1,000
anti-HSC70	sc-7298, Santa Cruz	1:2,000
anti-MAU2	ab183033, Abcam	1:1,000
anti-NIPBL	A301-779A, Bethyl	1:10,000
anti-Rad21	ab992, Abcam	1:1,000
anti-RPB1	ab817, Abcam	1:500
anti-RNAPI	sc-48385, Santa Cruz	1:200
anti-RNAPIII	ab88243, Abcam	1:1,000
anti-RNAPII^{Ser5}	61086, Active Motif	1:1,000
anti-SMC1A	ab9262, Abcam	1:4,000
anti-WAPL	16370-1-AP, Proteintech	1:1,000
anti-βTubulin	T0198, Sigma-Aldrich	1:2,000

Table S2. Lists of loops called in the different Hi-C datasets (*.xlsx* file).

Table S5. Significantly differentially-expressed genes in auxin-treated DLD-1 or HCT116 cells (*.xlsx* file).